MNHMT2013-22161

AN AB INITIO MOLECULAR DYNAMICS SIMULATION OF FEMTOSECOND LASER PROCESSING OF GERMANIUM

Pengfei Ji and Yuwen Zhang
Department of Mechanical and Aerospace Engineering
University of Missouri
Columbia MO 65211, USA
Email: zhangyu@missouri.edu

ABSTRACT

An ab initio molecular dynamics study of femtosecond laser processing of germanium is presented in this paper. The method based on the finite temperature density functional theory is adopted to probe the nanostructure change, thermal motion of the atoms, dynamic property of the velocity autocorrelation, and the vibrational density of states. Starting from a cubic system at room temperature ($300\ K$) containing 64 germanium atoms with an ordered arrangement of $1.132\ nm$ in each dimension, the femtosecond laser processing is simulated by imposing the Nose Hoover thermostat to the electron subsystem lasting for $\sim100\ fs$ and continuing with microcanonical ensemble simulation of $\sim200\ fs$. The simulation results show solid, liquid and gas phases of germanium under adjusted intensities of the femtosecond laser irradiation. We find the irradiated germanium distinguishes from the usual germanium crystal by analyzing their melting and dynamic properties.

1. INTRODUCTION

Femtosecond laser processing has been widely used in the fabrication process of cutting-edge semiconductor integrated circuits (ICs) and nanoelectromechanical systems (NEMS). Photolithography, serving as a conventional approach to fabricate the microstructures, has been a predominant technique since the emergent of semiconductors. However, traditional photolithography suffers from the drawbacks of high cost and complex treatment for the masks with the miniaturization of structure due to optical diffraction in nanoscale. Femtosecond laser processing (nanolithography), due to its inherent advantages of maskless super resolution [1], offers a potential solution for the high mask cost. In addition, compared with the nanosecond pulses, femtosecond laser has the advantages of high peak power intensity and a relatively smaller heat-affected zone, which make it ideal for a wide range of applications in other fields of material sciences. In many engineering applications ranging from laser micromachining to surface treatment, the femtosecond laser material interaction has become an increasingly hot topic. The laser intensity of femtosecond laser can even be up to $10^{21}\ W/m^2$ [2], which results in the breaking down of traditional phenomenological laws. Hence, for the purpose of achieving a better comprehension and understanding of the femtosecond laser nanolithography, it is of great necessity to investigate the melting and dynamic effects relating with energy transfer and conversion in the atomic scale.

For the femtosecond laser, the pulse duration is shorter than electron-lattice thermalization time (in the order of picosecond). Because the excited electrons do not have sufficient time to transfer a large amount of energy to the ions, plasma annealing seems to be the dominating mechanism. The ultrashort laser pulse makes it possible to excite the electronic states of a solid long before the appreciable energy transporting to the lattice vibrational states. Shank *et al.* [3] showed transition from crystalline order to disorder with melting of the surface occurred in less than $1\ ps$ under $90\ fs$ laser illumination on silicon. Rousse *et al.* [4] reported the nonthermal melting process in InSb at femtosecond resolution by using a ultrafast time resolved X-ray diffraction.

In this work, ab initio molecular dynamics simulation method based on finite temperature (FT-DFT) is used to simulate femtosecond laser interaction of germanium. The approach has already been employed to simulate the laser melting of silicon and graphite [5,6]. The original work of ab initio molecular dynamics of excited electrons was presented by Alavi *et al.* [7]. We carried out simulation with different incident laser intensities of $\sim100\ fs$ time duration.

2. MODELING AND SIMULATION

The ab initio molecular dynamics simulation was started with germanium crystal at room temperature ($300\,K$). The Car-Parrinello Molecular Dynamics (CPMD) package 3.15.3 [8] based on plane wave persudopotential implementation of FT-DFT and incorporating self-consistently the effects of thermal electronic excitations and fractionally occupied states was used. A cubic system containing 64 germanium atoms were modeled within $11.316\,Å$ at x-, y- and z- directions, which corresponds to the density of germanium at $5.323\,g/cm^{-3}$. The simulation time step was set $4\,a.u.$ ($\sim 0.096,755\,fs$). The exchange correlation in our simulation was represented by the local density approximation (LDA). We adopted the norm conserving pseudopotentials with Stumf-Gonze-Scheffler pseudolization method. Periodic boundary conditions were applied in all three directions of the primitive cell of diamond cubic crystal structure.

In order to perform FT-DFT simulation, wavefunction optimization and geometric optimization were performed first to calculate the electronic structure of the system. After obtaining the optimized electronic structure, all the cases were run for $1,000$ time steps at room temperature ($300\,K$) with Nose Hoover thermostats imposed on each degree of freedom for both electrons and nuclei, so that the electron subsystem and ion subsystem could reach to sufficient equilibrium state before laser irradiation.

Two typical treatments adopting constant temperature of electron subsystem are laser melting of silicon [5] for $0.4\,fs$ and graphite [6] for $0.5\,fs$. It can also be seen in the investigation of crystal stability in the density functional perturbation theory calculations [9] and ab initio molecular dynamics simulation of femtosecond laser interaction with vitreous silica [10]. In addition, as reported in the estimations of experiments, the electron temperature can be as high as $100,000\,K$ [6]. Therefore, we carried out simulation of femtosecond laser irradiation by instantly increasing the electron temperature to $20,000\,K$, $25,000\,K$, $30,000\,K$, $35,000\,K$, $40,000\,K$, $50,000\,K$ and $60,000\,K$ from the $1,001th$ to $2,000th$ time steps, which corresponded to the time duration of $\sim 100\,fs$.

The evaluation of electron temperature was based on the Maxwell-Boltzmann distribution of electron gas

$$\langle E \rangle = \frac{3k_B}{2}\langle T \rangle \qquad (1)$$

Therefore, the conversion of electron temperature at $1K$ in terms of the energy of $8.6173 \times 10^{-5} eV$ is used in the thermostats for temperature control. In this study, the instant incident of laser fluence can be expressed by the energy increment of electron subsystem.

$$\Phi = \frac{N_e N_I c \Delta T}{d_x d_y} \qquad (2)$$

where N_I and N_e refer to the number of atoms included in the system and the number of electrons circling around one germanium nuclei; c is the conversion coefficient from electron temperature to average electron energy; ΔT is the electron temperature increase induced by laser irradiation; and d_x, d_y are the width and length of the modeled system. The calculated average electron energy, laser fluence and laser intensity is listed in Table 1.

Table 1

Case	Electron Temperature (K)	Average Electron Energy (eV)	Laser Fluence (J/cm^2)	Laser Intensity ($10^{12}\,W/cm^2$)
1	20000	1.7235	0.0434	0.4490
2	25000	2.1543	0.0545	0.5630
3	30000	2.5852	0.0655	0.6769
4	35000	3.0161	0.0765	0.7908
5	40000	3.4469	0.0875	0.9048
6	50000	4.3086	0.1096	1.1328
7	60000	5.1704	0.1316	1.3607

3. RESULTS AND DISCUSSIONS

3.1 Temperature Evolutions

We calculated the temperatures of the ionic subsystems along with the MD simulation for all the cases. As is shown in Fig. 1, the phase change of melting and evaporation occurred around the electron temperature conditions of $25,000\,K$ and $50,000\,K$.
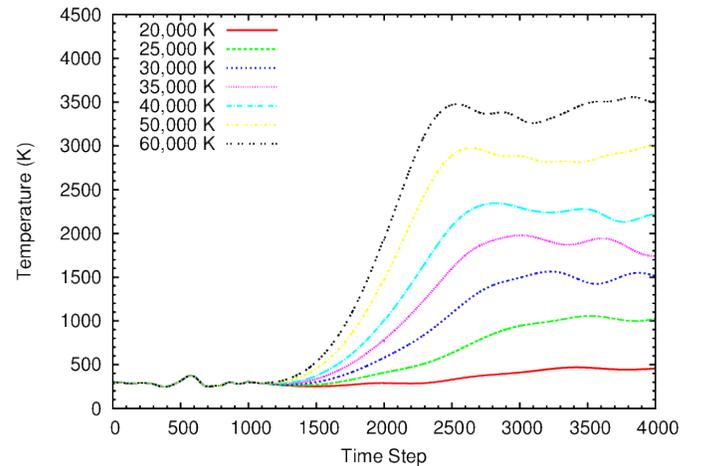
Fig. 1 Ion temperatures

As we can see from Fig. 1, the lattices remain at relatively lower temperatures in the first $1,000$ time steps of laser irradiation. When the condition of femtosecond laser interaction is imposed, the relatively low temperature states of ions keep about 200 time steps ($\sim 0.2\,fs$) and then are followed by slow temperature increments from $1,200$ to $1,500$ time steps. After $1,500$ time steps, the ion temperatures show abrupt increases, especially for cases of the electronic subsystems with relatively higher energies. The advents of ion temperatures exceeding the

melting and boiling points are also early for the electron systems with higher temperatures than those with lower electron temperatures. After the temperatures of ion subsystems increasing to certain values, they stayed and oscillated in small ranges at temporarily equilibrium states with the electron subsystems. The temperature curve $(1,000 - 4,000$ time steps) for the case of $20,000\,K$ is distinctly different from that of $25,000\,K$, which indicates that for the case of $20,000\,K$ femtosecond laser almost cannot make the ions to break most of the valence bonds connecting them but only keep with wild oscillations around their equilibrium positions. The same condition of femtosecond laser distinct threshold of $0.15\,J/cm^2$ that enables the strong excitation and nonthermal process was experimentally measured for femtosecond processing of gallium arsenide [11]. It is not definite to draw the final conclusion that the ions will still keep at low temperatures for the case of electron temperature $20,000\,K$, with the time duration to picosecond time scale. As pointed in Lindemann's law, once the vibrational amplitude reaches up to 10% of the nearest neighbor distance, the vibration will disrupt the equilibrium crystal lattice and the melting phenomenon eventually takes place. The short simulation period could not reveal the melting phenomena for this case. Nevertheless, we can find that even though the simulation process lasts for $\sim 0.3\,ps$, the temperature evolutions for the seven cases still distinguish from each other and the ion temperatures are much lower than the corresponding electron temperatures for all the cases. The phenomena can be interpreted from two aspects. On one hand, the incident energy heats the electrons more strongly than the ions. On the other hand, atoms and ions are much heavier than electrons, which lead to the inefficient thermal energy transfer in a two-body collision because the masses are dissimilar. Moreover, as computed in Table 1, the laser fluence exciting electron temperature to $60,000\,K$ is $0.1316\,J/cm^2$, which is in the same order of magnitude as reported for the femtosecond laser ablation threshold fluence $(0.2\,J/cm^2)$ for silicon [12].

3.2 Nanostructure Change due to Melting and Evaporation
To understand the melting effect of femtosecond laser nanolithography, the nanostructure change is the primary parameter to evaluate the results of irradiated germanium. The Radial distribution functions (RDFs) for the room temperature were calculated first and the results are shown in Fig. 2. It can be clearly seen that there are peaks and valleys, which reflect the regular arrangement of germanium atoms in the crystal at room temperature. In order to obtain the information of solid, liquid and gas phases, we chose the cases with electron temperatures of $20,000\,K$, $30,000K$ and $60,000\,K$ to calculate the RDFs for comparison (see Figs. 3-5). The temporarily stable ion temperatures for the three cases are approximately $400K$, $1,500\,K$ and $3,500\,K$, respectively. We also computed the RDFs for germanium in three phases (corresponding to $400K$, $1,500\,K$ and $3,500\,K$) that the electron temperature and ion temperature are the equal (see the purple curves in Figs. 3-5). The maximum distance in real
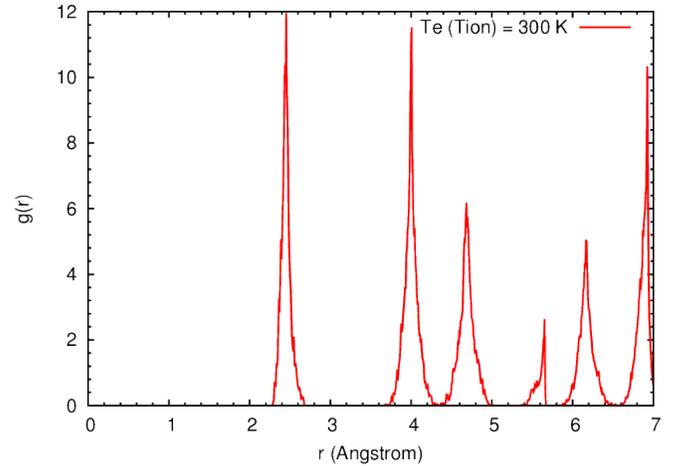

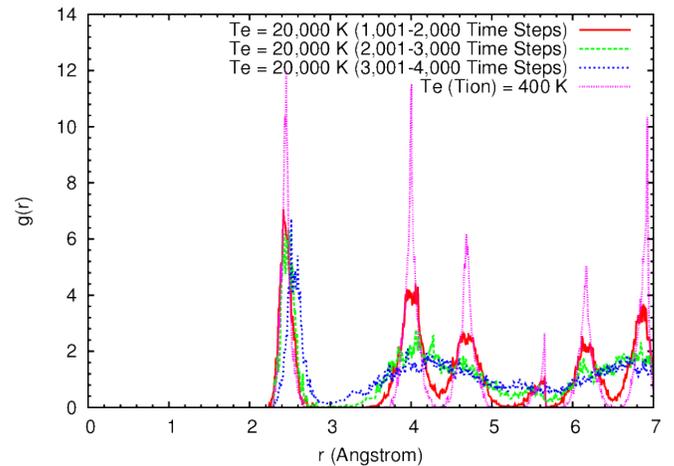Fig. 2 RDF of germanium crystal at room temperature (300 K)

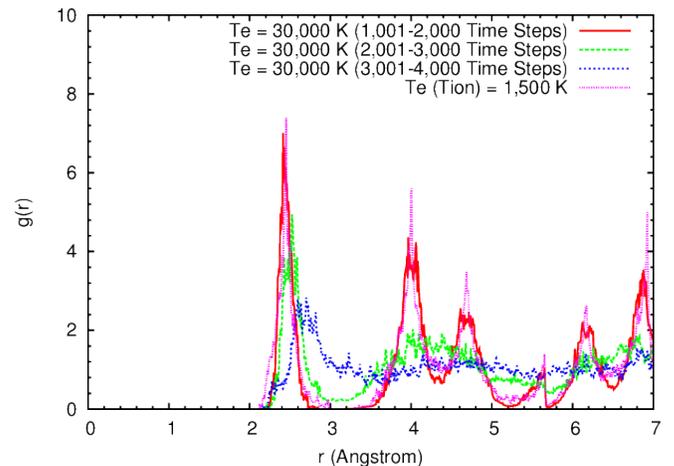**Fig. 3** RDFs at different stages, solid state (20,000 K)

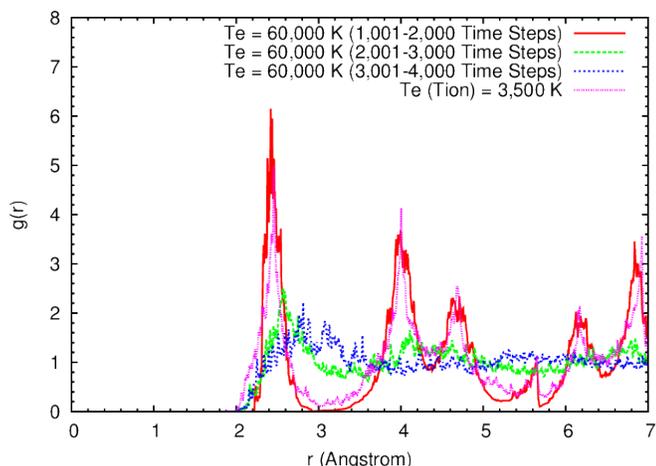**Fig. 4** RDFs at different stages, liquid state (30,000 K)
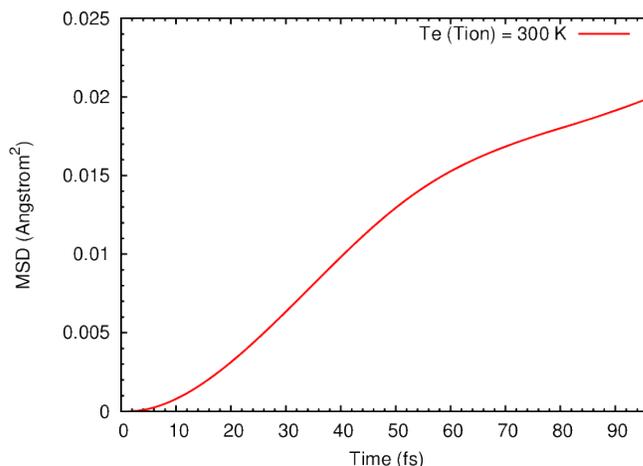
Fig. 5 RDFs at different stages, gas phase (60,000 K)

Fig. 6 MSD of germanium crystal at room temperature

Fig. 7 MSDs at different stages, solid state (20,000 K)

Fig. 8 MSDs at different stages, liquid state (30,000 K)

germanium at difference phases with selected stages like Section 3.2.

space to sample the number of germanium atoms was chosen to be 7 Å. Due to the abrupt shock of high level energy in the electronic subsystem, the nanostructure of germanium is disturbed since the initial irradiation stage of femtosecond laser. The emergences broadening peaks and valleys from $1,001-2,000$ time steps to $2,001-3,000$ time step then to $3,001-4,000$ time steps indicate the germanium atoms are gradually ionized. Because the RDFs in Figs. 3-5 represent distinctly differently phase states, the shapes and values correspondingly distinguish from each other. The differences of occurrences for the three cases reveal the atomic distances are separated due to the shock of incident lasers. With the higher intensity, the more random distribution of atom occurs (see the valleys in the red curves in Fig. 4 and Fig. 5). But due to the atomic separation, the maximum peak that shows the greatest probability of finding atoms at short distance) is consequently moves to larger atomic distance (see the first peak of different stages in Figs. 5, 6 and 7. For the case of electron temperature 20,000 K, comparing the red curve with the green and blue curves, we can see that even though the crystal is not melted by the hot electrons, the nanostructure has already changed. As seen in Fig. 1, the temporarily stable temperature of the case 20,000 K is around 400K.

Thus, to make the prediction even more persuasive, we calculated the RDF of germanium, whose temperatures of electron subsystem and the ion subsystem are both set as 400 K (see the purple curve in Fig. 3). The profile of the purple curve ($T_{e\&I} = 400\,\text{K}$) in Fig. 3 resembles the curve ($T_{e\&I} = 300\,\text{K}$) in Fig. 2, which indicates atoms in the solid germanium are kept as ordered arrangements. In addition, the comparisons between the purple curve and the red curve, because the ion temperatures are approximately equal and the irradiation initially starts, the RDF results show the almost overlapping profiles.
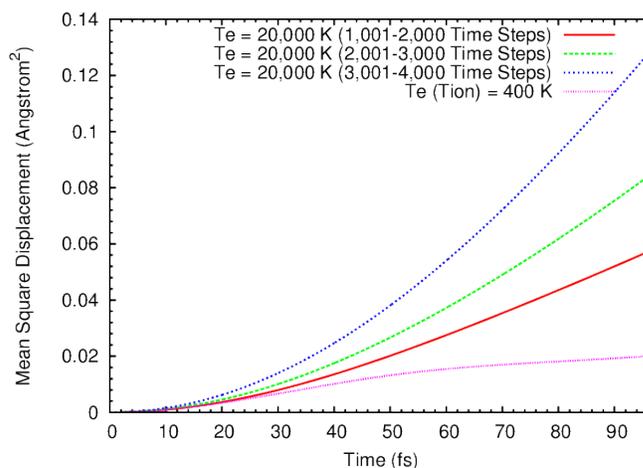
3.3 Thermal Motion of Atoms

To quantitatively measure the extent of spatial random motion of the atoms, we calculated the mean square displacement (MSD) of the atomic thermal motion for
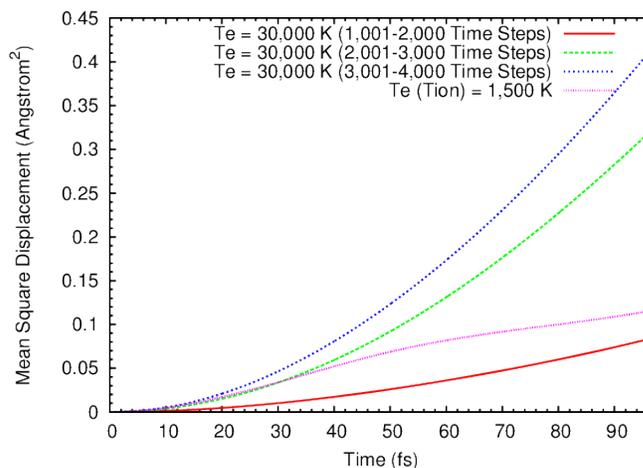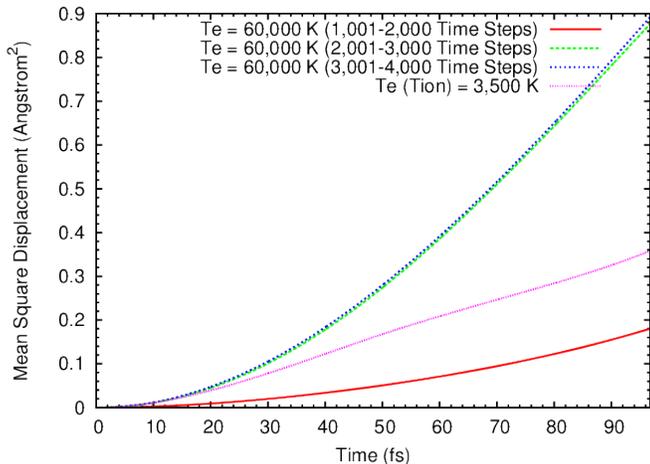
Fig. 9 MSDs at different stages, gas state (60,000 K)

Figure 6 shows the calculated MSD of the solid state germanium and the value at the end of the 1,000 time steps (96.755 fs) is about $0.02 \, \text{Å}^2$. Because the thermal motion of atoms is only characterized by phonon vibrations, there is no appreciable MSD. In Figs. 7-9, the calculated MSDs of different simulation stages since the femtosecond laser irradiation are plotted. A general tendency of increasing values at the ending point of each 1,000 time steps is revealed in Figs. 7-9. In addition, for the cases of higher electron temperature, the MSD magnitudes are correspondingly higher. The discrepancies of purple curves between the other three curves verify the predication that germanium with equal electron temperature and ion temperature is different from the ones that the electrons are excited. Moreover, the slope of red curve in Fig. 7 is relatively steeper than the purple curve in Fig 7. Thus, we can see that the motion property of the laser irradiated germanium is more like fluids rather than the germanium with same temperature at the solid state. The remarkably high energy femtosecond laser irradiated MSD is also reported for vitreous silica [10], whose ion temperature is $\sim 500 \, K$ after irradiation. The other point that deserves our attention is the red curves in each of Figs. 7-9, when they are compared with the green and blue curves. We can find that in Fig. 7, the final value of red curve MSD is $0.135 \, \text{Å}^2$. However, the squared distance of thermal motion of the green one in Fig. 7 is more than 1.73 times of that in red. In addition, the ratio of the final value between blue cure and green curve gradually narrow down from Figs. 7 to 9. In Fig. 9, the blue curve and green curve are almost coincide with each other, which indicates the nonthermal melting of laser irradiated germanium thoroughly developed in the $2,001 - 3,000$ time steps and there are no significant differences distinguishing from the subsequent $3,001 - 4,000$ time steps.

4. CONCLUSION

Ab initio molecular dynamics study of the thermal and dynamic effect induced by femtosecond laser irradiation is performed in this paper. By employing the finite temperature density functional theory and incorporating with direct energy minimization, the accurate pseudopotential description of core electrons and the Nose Hoover dynamics temperature control of the electronic and ionic subsystem, our simulation successfully obtained the results of the germanium in three phases (solid, liquid and gas). The nanostructures and maximum value of the atomic thermal motion depend on the excited levels of the thermalized electrons. The melting and dynamic response of ionic system also depends on the incident laser intensity, which means the higher excited electronics subsystem, the rapider temperature response of the ionic subsystem. However, there are some thresholds for the energy of the electron subsystem that limits the phase change from solid to liquid and liquid to gas phase. The occurrences of melting and evaporation are determined by both the electronic and the ionic subsystems.

Our work demonstrates the great potential of ab initio MD simulation of the nanostructure materials. With the advantages over classical MD simulation that interatomic potential empirically defined and other numerical modeling and simulation methodologies, it is possible to broaden the ab initio MD simulation to thermodynamical problems involving the participation of electron interaction and transport in the future.

REFERENCES

[1] Koch J., Fadeeva E., Engelbrecht M., Ruffert C., Gatzen H. H., Ostendorf a., and Chichkov B. N., 2005, "Maskless nonlinear lithography with femtosecond laser pulses," Applied Physics A, **82**(1), pp. 23–26.

[2] Zhang Y., and Chen J. K., 2007, "Melting and resolidification of gold film irradiated by nano- to femtosecond lasers," Applied Physics A, **88**(2), pp. 289–297.

[3] Shank C., Yen R., and Hirlimann C., 1983, "Femtosecond-time-resolved surface structural dynamics of optically excited silicon," Physical Review Letters, **51**(10), pp. 900–902.

[4] Rousse A., Rischel C., Fourmaux S., Uschmann I., Sebban S., Grillon G., Balcou P., Forster E., Geindre J. P. P., Audebert P., Gauthier J. C. C., Hulin D., and Förster E., 2001, "Non-thermal melting in semiconductors measured at femtosecond resolution.," Nature, **410**(6824), pp. 65–8.

[5] Silvestrelli P. L. P., Parrinello M., Alavi A., and Frenkel D., 1996, "Ab initio Molecular Dynamics Simulation of Laser Melting of Silicon," Physical Review Letters, **77**(15), pp. 3149–3152.

[6] Silvestrelli P. L., and Parrinello M., 1998, "Ab initio Molecular Dynamics Simulation of Laser Melting of Graphite," Journal of Applied Physics, **83**(5), p. 2478.

[7] Alavi A., Kohanoff J., Parrinello M., and Frenkel D., 1994, "Ab Initio Molecular Dynamics with Excited Electrons," Physical Review Letters, **73**(19), pp. 2599–2602.

[8] "CPMD," http://www.cpmd.org/, Copyright IBM Corp 1990-2008, Copyright MPI fur Festkorperforschung Stuttgart 1997-2001.

[9] Recoules V., Clérouin J., Zérah G., Anglade P., and Mazevet S., 2006, "Effect of Intense Laser Irradiation on the Lattice Stability of Semiconductors and Metals," Physical Review Letters, **96**(5), p. 055503.

[10] Sen S., and Dickinson J., 2003, "Ab initio molecular dynamics simulation of femtosecond laser-induced structural modification in vitreous silica," Physical Review B, **68**(21), p. 214204.

[11] Sokolowski-Tinten K., and Bialkowski J., 1998, "Thermal and nonthermal melting of gallium arsenide after femtosecond laser excitation," Physical Review B, **58**(18), pp. 11805–11808.

[12] Bonse J., Baudach S., Krüger J., Kautek W., and Lenzner M., 2002, "Femtosecond laser ablation of silicon-modification thresholds and morphology," Applied Physics A, **25**(74), pp. 19–25.